Title
Diode laser-induced fluorescence measurements of metastable argon ions in a magnetized inductively coupled plasma

Journal
Physics of Plasmas, 13(5)

ISSN
1070-664X

Authors
Jun, S
Chang, HY
McWilliams, R

Publication Date
2006-05-01

DOI
10.1063/1.2201894

Diode laser-induced fluorescence measurements of metastable argon ions in a magnetized inductively coupled plasma

S. Jun and H. Y. Chang
Department of Physics, Korea Advanced Institute of Science and Technology, 373-1, Guseong-dong, Yuseong-gu, Daejeon 305-701, South Korea

R. McWilliams
Department of Physics and Astronomy, University of California, Irvine, California 92697-4575

(Received 8 November 2005; accepted 11 April 2006; published online 22 May 2006)

Velocity distribution functions of metastable argon ions ($3d'^4F_{7/2}$) have been measured to obtain metastable ion density and temperature by the diode laser-induced fluorescence (LIF) technique in magnetized inductively coupled plasma as a function of pressure, rf power, and magnetic field strength. Calculated density from a rate equation agrees with the trends observed in the experimental data. From the calculation, the metastable ion density should be over 10^7 cm^{-3} to obtain a LIF signal. From a dc bias experiment, it is suggested that the spatial potential can be the dominant ion heating source, and a simple global model for ion temperature is constructed. In this model, approximately 0.01% and 10% of total spatial potential energy can contribute to ion and neutral temperatures, respectively. The measured ion temperature agrees with the calculation.
 [DOI: 10.1063/1.2201894]

I. INTRODUCTION

Laser-induced fluorescence (LIF) was first applied to plasma in the 1970s.[1,2] Since then, it has been one of the most powerful diagnostics for the detection of ions, neutrals and radicals in the plasma. Since the 1980s, high power, single mode, tunable dye lasers have been used widely for laser induced fluorescence measurements.[3] In 1998, Severn *et al.* had success in making a new LIF measurement scheme of metastable argon ions at 668.61 nm with a diode laser.[4] A diode laser has many advantages such as a lower cost, easier maintenance, and better day-to-day stability when compared with a dye laser.[5] This new scheme combined of two lasers, a New Focus Vortex 6009 laser as a seed laser and an SDL 8630 laser as an amplifier. Recently, Boivin and Scime determined that a different, newer diode laser also works for 668.61 nm argon LIF.[6,7]

LIF has been used widely to measure ion or neutral density, temperature and velocity distribution functions in order to understand ion or neutral dynamics in tokamak plasma,[8,9] multidipole filament plasma,[10,11] ICP,[12–16] helicon plasma,[17–20] ECR plasma,[21–23] etc. LIF has such good spectral resolution (~0.0025 eV ion or neutral temperature)[10] that many experiments on ion or neutral heating have been conducted in low-temperature processing plasmas. These efforts explained ion heating qualitatively from electron-ion collisions,[17] potential in the presheath,[13,21] and wave interaction,[18] but these were not enough to explain why ion temperature is much higher than room temperature in the center of the plasma. In this study, we have used the diode LIF scheme to measure metastable argon ion velocity distribution functions in magnetized inductively coupled plasma to obtain metastable ion density and temperature. Metastable ion density is estimated from a simple rate equation. We also suggest ion and neutral heating by spatial potential, and construct a model to explain why the ion temperature in the center of the plasma can be much higher than room temperature qualitatively and quantitatively.

II. EXPERIMENTAL SETUP

All experiments were performed in a magnetized inductively coupled plasma chamber (Fig. 1), which consisted of a Pyrex tube that was 110 mm in diameter and 230 mm long and a stainless steel chamber that was 220 mm in diameter and 600 mm long. A single-turn antenna was placed at 70 mm from the top of the Pyrex tube. Two coil magnets generated a static magnetic field. A grounded electrode, which was 200 mm in diameter, was movable and controlled the plasma volume. The plasma length in the stainless steel chamber was fixed at 250 mm. The plasma was generated at 13.56 MHz at all conditions with various pressures, rf powers, and magnetic field strengths.

The Vortex 6009 tunable diode laser (New Focus, Inc.) as a seed laser and the modified SDL-8630 tunable laser diode (SDL, Inc.; now part of JDS Uniphase) as an amplifier were both used for the LIFmeasurements of the metastable argon ion.[4] The wavelength of the Vortex 6009, which has a linewidth of 500 kHz, was centered at 668.61 nm for the transition of $3d'^4F_{7/2} \rightarrow 4p^4D^0_{5/2}$. The resulting fluorescence was recorded at 442.72 nm for a $4p^4D^0_{5/2} \rightarrow 4s^4P_{3/2}$ transition. A cw diode laser beam was chopped at 1 kHz with a mechanical chopper and injected in the radial direction parallel to the electrode and perpendicular to the magnetic field. The laser power in the center of the chamber was approximately 20 mW. The resulting fluorescence was measured at 70 mm above the substrate and focused to a multimode fiber at a right angle through the collection optics, which included a 240 mm focal length lens, a 90 mm focal length lens, and a 1 nm bandwidth bandpass optical filter. The fluorescence

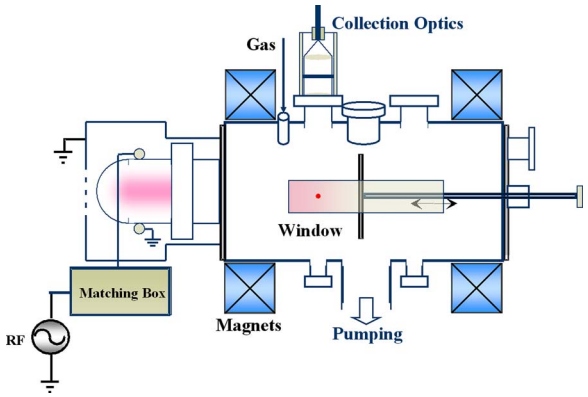

FIG. 1. MICP chamber.

was amplified by a photomultiplier (PM) tube and processed by a lock-in amplifier. The ion velocity distribution parallel to the direction of the laser beam was measured, and was fitted to a Maxwellian velocity distribution (Fig. 2). Metastable ion density and temperature were obtained from the area and the full width of half maximum (FWHM) of the distribution, respectively.

An rf-compensated Langmuir probe[24] was used to measure the electron density and temperature. The probe tip was made of 0.15 mm diam tungsten wire. 2 mm of the probe was exposed to the plasma. SLP2000 (Plasmart, Inc.)[25] was used to control the probe bias, and also to obtain and handle the signal of the *I-V* curve, the electron energy probability function (EEPF), the electron energy distribution function (EEDF), etc. The measured EEDF (or EEPF) was almost Maxwellian in all conditions.

III. RESULTS AND DISCUSSION

A. Theoretical model for metastable ion density

The metastable argon ions can be generated from direct electron-impact excitation of both ground state argon neutrals and ground state argon ions. But the metastable argon

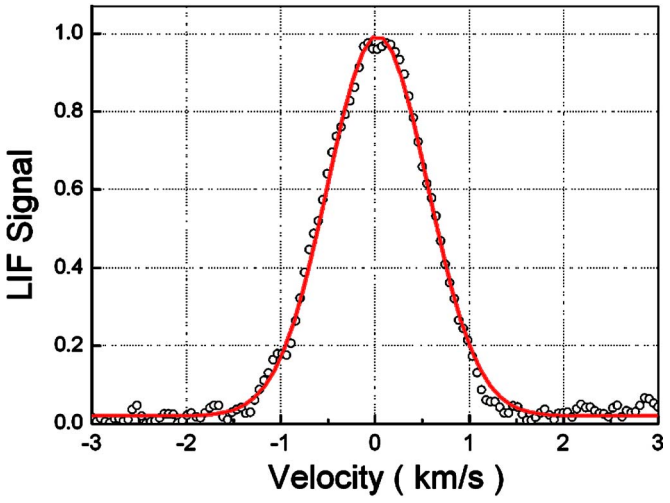

FIG. 2. Measured metastable ion velocity distribution function. LIF signal is normalized to 1. The solid line is a Maxwellian fit to the distribution function.

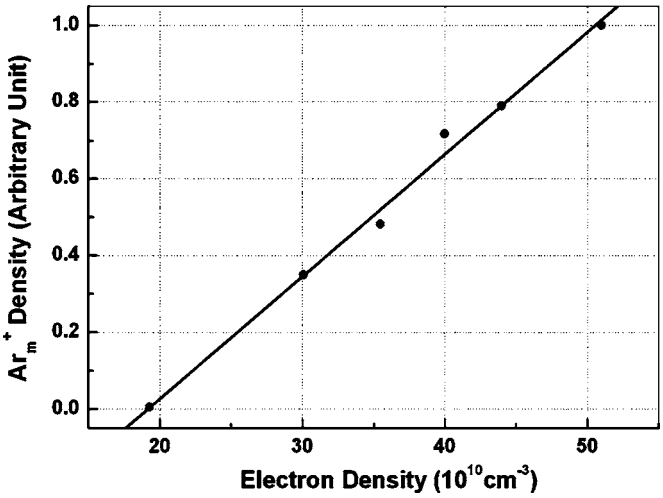

FIG. 3. Metastable ion density vs electron density when rf power changes. In this condition, the electron temperature is almost constant. Therefore, this linear relationship means that the dominant metastable ion generation is from the ground state neutral ionization.

ions are generated dominantly from the ground state argon neutrals in this experimental condition because metastable argon ion density is proportional to electron density when the electron temperature is constant in Fig. 3. The lifetime (τ) of this metastable ion ($3d'^4F_{7/2}$) is higher than 10 μs (Ref. 10) and we use τ as 10 μs. Because the ion temperature is approximately 0.1 eV, the metastable ions can travel ~1 cm during their lifetime. The neutral-metastable ion collisional quenching cross section for argon is 3×10^{-16} cm^2,[26] and its mean free path is approximately 1 m at 1 mTorr. Additionally, the neutral-metastable ion collisional quenching rate ($\sim n_n\sigma_{im,n}v_i$) is much lower than the lifetime decay rate ($=1/\tau$). Therefore, the lifetime decay is the dominant quenching loss mechanism for the metastable argon ions. The metastable ion density can be determined from a simple zero-dimensional rate equation [see Eqs. (1) and (2) below] with the above description. The electron-impact excitation rate coefficients from the ground state argon neutrals ($K_{\mathrm{ex}}^{e,n}$) is assumed to have the same form as the rate coefficient of the electron-impact excitation from a ground state to a metastable state of argon neutrals[27] [Eq. (3)]:

$$\frac{dn_{\mathrm{im}}}{dt} = K_{ex}^{e,n} n_e n_n - \frac{1}{\tau} n_{\mathrm{im}} \simeq 0, \tag{1}$$

$$\therefore n_{\mathrm{im}} \simeq \tau K_{\mathrm{ex}}^{e,n} n_e n_n, \tag{2}$$

$$K_{\mathrm{ex}}^{e,n} \sim \frac{10^{-8}}{\sqrt{T_e}} \exp\left(-\frac{33.45}{T_e}\right). \tag{3}$$

Figure 4 shows the electron density, electron temperature, and plasma potential as a function of pressure, rf power, and *B* field. Figure 5 shows the measured metastable ion density and calculated metastable ion density. Both of the densities are normalized to 1, and the measured relative metastable ion density can be calibrated to an absolute value. When the pressure increases in Fig. 5(a), the metastable ion density increases sharply and then decreases exponentially

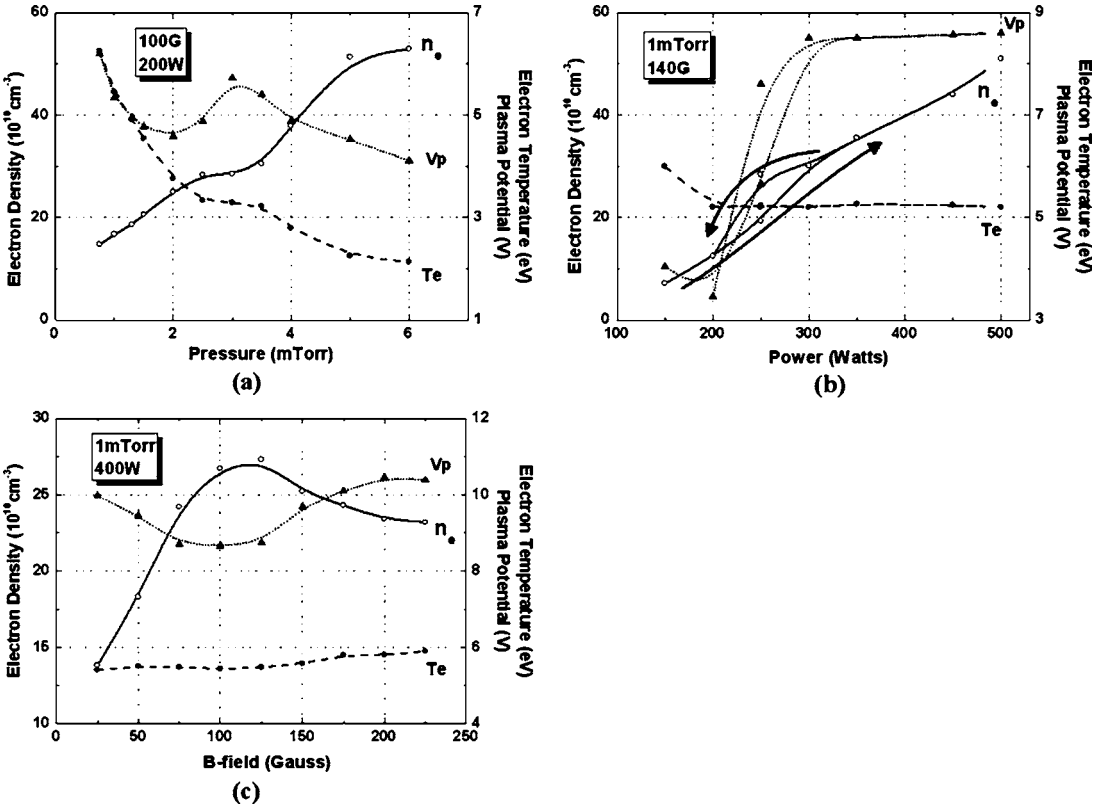

FIG. 4. Electron temperature, electron density, and plasma potential as a function of pressure, rf power, and B field.

even though the electron density increases. This is caused by the decrease of electron temperature and the exponential dependence of the production rate ($K_{\mathrm{ex}}^{e,n}$) to electron temperature. The calculated metastable ion density fits well with the experimental data, and the metastable ion density is approximately 10^7–10^9 cm^{-3} by the calculation. Above 5 mTorr, the LIF signal was not detected. This may be interpreted that the metastable ion density should be over $\sim 10^7$ cm^{-3} to detect the LIF signal in this diode laser operation. When rf power increases, the metastable ion density increases almost linearly, showing a hysteresis on a mode transition. This phenomenon is caused because plasma parameters show hysteresis and a mode transition, as seen in Fig. 4(b). The calculated ion density also shows hysteresis and increases with the power, but has a smaller increasing slope than the measured density. Here, the calculated metastable ion density is approximately 10^7–10^9 cm^{-3}. When the magnetic field increases from zero, the metastable ion density first increases. The metastable ion density starts to saturate at $B \sim 150$ G. The calculated metastable ion density is approximately 10^7–10^9 cm^{-3}.

This global modeling predicts metastable ion density well, but shows a small amount of deviation from the measurements. This calculation is sensitive to the electron temperature due to the exponential dependence of the production rate coefficients; therefore, an accurate measurement of the electron temperature is critical.

B. dc bias effect

We can consider that the ion heating sources are simply electron-ion collisions, the acceleration from spatial potential, and wave-particle interactions. Recently, Scime *et al.* suggested the electron-ion collision need not be the main ion heating source; instead, in a helicon plasma, slow wave heating may be dominant.[18] The ion temperature measured in an unmagnetized inductively coupled plasma also is approximately 0.1–0.3 eV.[12,15] Thus, it is thought that a wave may not be needed to explain the 0.1 eV temperature in our plasma source. Therefore, an attempt is made to note ion heating by an ion-ion collision and ion-neutral collision after acceleration from the spatial potential in a dc bias experiment. The metastable ion temperature is estimated to be the same as the ground state ion temperature.[12]

To see the spatial potential effect on ion heating, we applied a dc negative bias to the substrate. In Fig. 6, the electron temperature is almost constant and the plasma potential decreases with the increasing negative bias voltage. The total spatial potential from the bulk to the substrate increases with the bias voltage because the substrate is negatively biased, and the ion temperature in the bulk plasma increases. Consequently, we can conclude that spatial potential plays an important role in ion heating.[13,21] It may be doubted that the ion temperature increases due to the relative measurement position change in the presheath when biased. However, in this experiment this bias increases the total spatial potential including sheath potential in the axial direction,

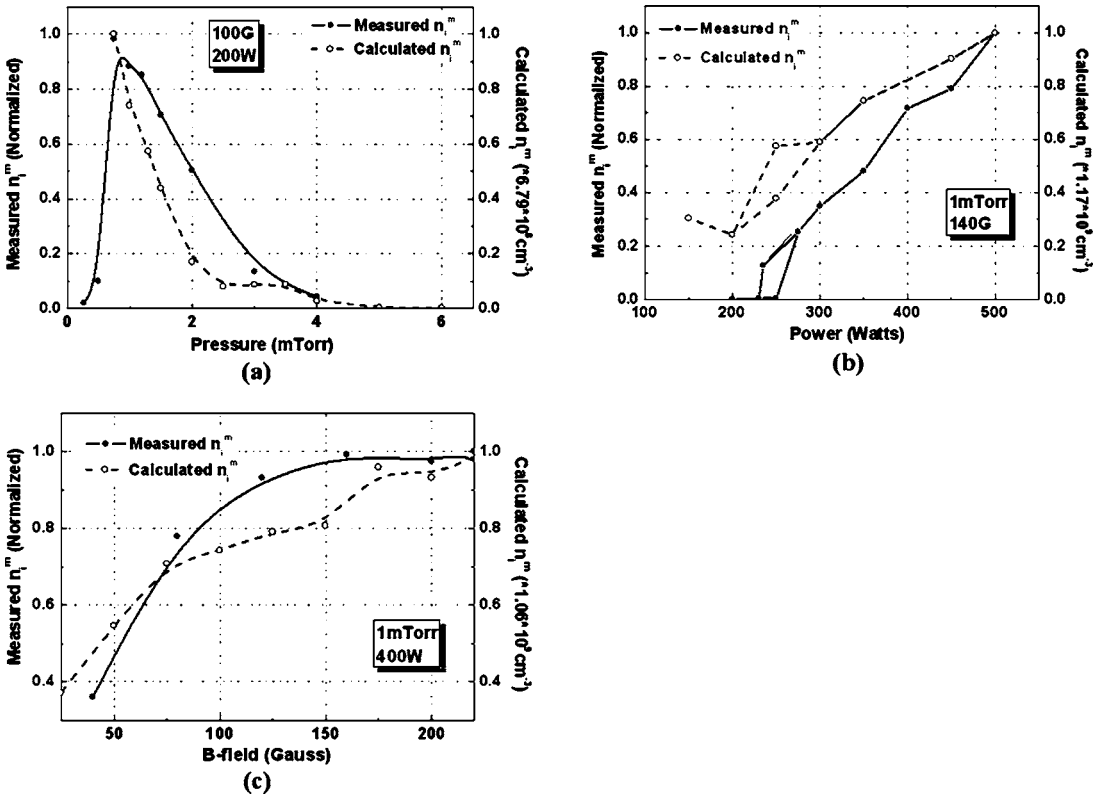

FIG. 5. Comparison between measured metastable ion density and calculated metastable ion density as a function of pressure, power, and B field. Both densities are normalized to 1.

but the ion temperature is measured in the radial direction. Even though the ion temperature in the axial direction is changed at different positions of the presheath, the ion temperature in the radial direction can be constant in the center of the plasma if it is far from the sheath in the axial direction.[13]

C. Theoretical model for ion temperature

Ions can be heated from electron-ion collisions, but the ion temperature calculated only with this term was almost the same as a wall temperature in the low temperature plasma. 0.1 eV of energy cannot be explained solely by this heating source term in this experiment. Now, we consider the additional heating source of the spatial potential. This mechanism progresses as follows: An ion becomes accelerated from a spatial potential to have an additional drift velocity. First, it can collide with other ions or neutrals and transfer some of its energy to those ions or neutrals. This thermalization increases the ion and neutral temperatures. Second, the accelerated ion can have a charge exchange collision with a neutral. In this case, the total ion energy including the drift energy from the acceleration is converted to neutral kinetic energy. This neutral is thermalized to increase the neutral temperature. This means that the spatial potential

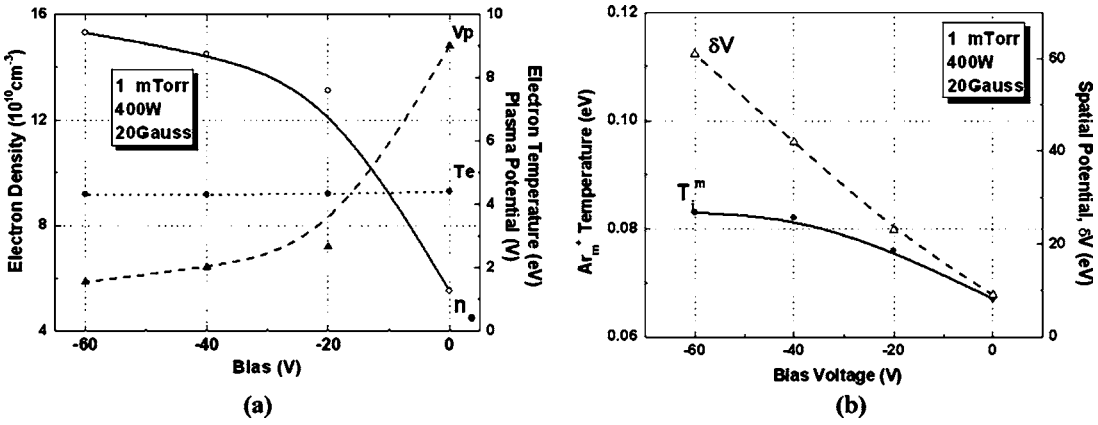

FIG. 6. (a) Electron temperature, electron density, and plasma potential vs bias voltage. (b) Ion temperature and total spatial potential, $\delta V(=V_p - V_{\text{bias}})$ vs bias voltage.

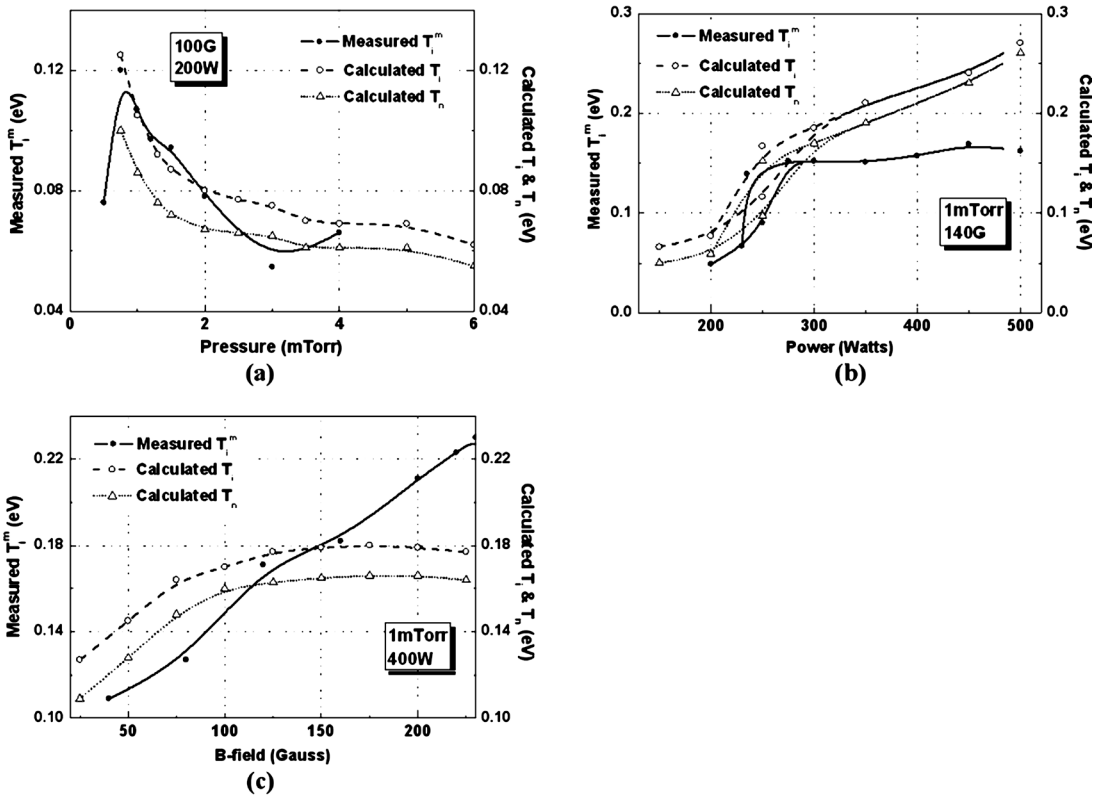

FIG. 7. Comparison between measured ion temperature and calculated ion temperature as a function of pressure, power, and B field. Neutral temperature is also calculated.

energy is converted to neutral temperature. The heated neutrals can be also ionized in the plasma bulk. Thus, the ion temperature in the bulk plasma can be high. Thus, ion heating is correlated with neutral heating in this analysis.

Ion and neutral temperatures are determined from energy balance equations [see Eqs. (4) and (5) below].[28] It is assumed that ions obtain energy from electron collisions (υ_{ei}) and the acceleration from spatial potential ($\Delta V = V_p - V_{\text{wall}}$), and they lose energy by neutral collisions (υ_{ni}) as well as wall collisions. Neutrals are assumed to obtain the same amount of energy that electrons and ions lose by the neutral collisions. In addition, it is assumed that neutrals lose energy through wall collisions. Because it is not clear how much spatial potential energy can contribute to ion and neutral temperatures, two contribution factors are introduced here: α and β. In Eqs. (6) and (7), the ion and neutral temperatures are also functions of the ion and neutral temperatures through the collision frequency. This equation cannot be solved simply. Initial values of $T_i[0]=0.03$, $T_n[0]=0.03$ were chosen and converging nth values were obtained by an iteration method. The wall temperature was fixed as $T_w=0.03$:

$$\frac{d(n_i T_i)}{dt} = \nu_{ei}\frac{3m}{M}n_e(T_e - T_i) + \nu_{ii}n_i(\alpha e\Delta V) - \nu_{in}n_i(T_i - T_n) - \frac{n_i \upsilon_{\text{Bohm}}}{R}(T_i - T_w) \simeq 0, \tag{4}$$

$$\frac{d(n_n T_n)}{dt} = \nu_{en}\frac{3m}{M}n_e(T_e - T_n) + \nu_{in}n_i(\beta e\Delta V + T_i - T_n) - \frac{\frac{1}{4}n_n \upsilon_n}{R}(T_n - T_w) \simeq 0, \tag{5}$$

$$T_i = \frac{\nu_{ei}\frac{3m}{M}n_e T_e + \nu_{ii}n_i(\alpha e\Delta V) + \nu_{in}n_i T_n + \frac{n_i \upsilon_{\text{Bohm}}}{R}T_w}{\nu_{ei}\frac{3m}{M}n_e + \nu_{in}n_i + \frac{n_i \upsilon_{\text{Bohm}}}{R}}, \tag{6}$$

$$T_n = \frac{\nu_{en}\frac{3m}{M}n_e T_e + \nu_{in}n_i(\beta e\Delta V + T_i) + \frac{n_n \upsilon_n}{4R}T_w}{\nu_{en}\frac{3m}{M}n_e + \nu_{in}n_i + \frac{n_n \upsilon_n}{4R}}. \tag{7}$$

The metastable ion temperature was also measured as a function of pressure, rf power, and magnetic field (Fig. 7) with approximately ±10% error. The ion temperature increases sharply at a lower pressure than 0.7 mTorr, and decreases with pressure due to a charge exchange collisional loss, as shown in Fig. 7(a). This is calculated from Eqs. (6) and (7) with $\alpha=0.0001$ and $\beta=0.1$ to obtain 0.1 eV ion temperature. However, the calculated ion temperature increases as the pressure increases with a constant α and β. We found that the contribution factors, α and β, decrease with the pres-

sure to match the calculated temperatures to the experimental results. The calculation is well fitted to the measured ion temperature after the substitution of α with α/p (p in mTorr). The ion and neutral temperatures in Fig. 7 are calculated from modified equations (8) and (9):

$$T_i = \frac{\nu_{ei}\frac{3m}{M}n_e T_e + \nu_{ii}n_i\left(\frac{\alpha}{p}e\Delta V\right) + \nu_{in}n_i T_n + \frac{n_i v_{\mathrm{Bohm}}}{R}T_w}{\nu_{ei}\frac{3m}{M}n_e + \nu_{in}n_i + \frac{n_i v_{\mathrm{Bohm}}}{R}}, \tag{8}$$

$$T_n = \frac{\nu_{en}\frac{3m}{M}n_e T_e + \nu_{in}n_i\left(\frac{\beta}{p}e\Delta V + T_i\right) + \frac{n_n v_n}{4R}T_w}{\nu_{en}\frac{3m}{M}n_e + \nu_{in}n_i + \frac{n_n v_n}{4R}}. \tag{9}$$

The neutral temperature is also calculated simultaneously with the ion temperature, and has a slightly lower value than the ion temperature. The neutral temperature shows nearly the same trend as the ion temperature because neutral heating is related to ion heating. However, because of a lack of measured data on neutral temperature, it is not known whether the calculated neutral temperature is correct or not compared to the actual value. However, it is possible to find a neutral temperature similar to the ion temperature in some investigations.[12,15] The ion temperature increases with the rf power and magnetic field strength, as seen in Figs. 7(b) and 7(c). In particular, the ion temperature shows hysteresis with the rf power. This is because the plasma density and plasma potential have hysteresis. Calculated ion temperatures show a small amount of deviation compared to the experimental results. It appears that α and β may depend on certain other parameters in addition to pressure. However, it is not yet apparent what these dependencies are.

Finally, it can be said that the ion temperature increases linearly with the total spatial potential in this model. But the ion heating by the potential is related to the ion density multiplied by the potential. Therefore, even if the total spatial potential decreases, increasing the ion density can increase the ion temperature. Thus, the calculated ion temperature seems to be following the value of the ion density multiplied by the potential due to the use of the constants, α and β. However, it is necessary to determine the parameter dependencies of α and β. Additionally, it is expected that $\Delta V/p$ can be replaced as $\int[E(\vec{r})/p]d\vec{r}$ in the n-dimensional ($n=1,2,3$) simulation, but additional terms like spatial energy transport should be needed in that case. The measured metastable ion temperature can be thought to be the same as neutral temperature because we concluded that the metastable ions are generated from direct excitation of ground state neutrals in Sec. III A. But the ion temperature is almost the same as the neutral temperature in the center of the plasma in this analysis. If LIF is measured in the presheath or sheath, metastable ion temperature may not be the same as ion temperature.

IV. CONCLUSION

A metastable argon ion ($3d'^4F_{7/2}$) density and temperature are measured as a function of pressure, rf power, and magnetic field by a diode LIF method in magnetized inductively coupled plasma. Global models are constructed to calculate metastable ion density and temperature. Metastable argon ions are generated from direct electron-impact excitation of ground state neutrals, and they are dominantly lost by lifetime decay. The relative changes in the calculated ion density and temperature follow the trends of the experimental results. By this calculation, the metastable argon ion ($3d'^4F_{7/2}$) density is approximately 10^7-10^9 cm^{-3}, and the metastable ion density must be larger than approximately 10^7 cm^{-3} in order to obtain a LIF signal with this diode LIF scheme in this experiment. In a dc bias experiment, the spatial potential may be the main ion and neutral heating source rather than the phenomenon of electron collisions. As we still do not know how much potential energy would contribute to the ion and neutral temperatures, we introduced the contribution factors, α and β, for initial models. As a result, $0.01\%(=\alpha)$ and $10\%(=\beta)$ of spatial potential energy was shown to contribute to ion and neutral temperatures. It may be interesting to consider further dependencies of α and β on such parameters as pressure.

ACKNOWLEDGMENTS

The authors would like to thank the Korea Basic Science Institute Hanbit User's Program and the Tera-level Nano-Devices project of MoST (TND, Grant No. M103KC010008-05K0301-00820) for their financial supports. In addition, we thank the National Fusion Research Center of Korea for the lending of the diode laser system.

[1] D. D. Burgess and C. H. Skinner, J. Phys. B **9**, 297 (1974).
[2] R. A. Stern and J. A. Johnson III, Phys. Rev. Lett. **34**, 1548 (1975).
[3] D. N. Hill, S. Fornaca, and M. G. Wickham, Rev. Sci. Instrum. **54**, 309 (1983).
[4] G. D. Severn, D. A. Edrich, and R. McWilliams, Rev. Sci. Instrum. **69**, 10 (1998).
[5] C. E. Weiman and L. Hollberg, Rev. Sci. Instrum. **62**, 1 (1990).
[6] R. F. Boivin and E. E. Scime, Rev. Sci. Instrum. **74**, 4352 (2003).
[7] A. M. Keesee, E. E. Scime, and R. F. Boivin, Rev. Sci. Instrum. **75**, 4091 (2004).
[8] J. M. McChesney, R. A. Stern, and P. M. Bellan, Phys. Rev. Lett. **59**, 1436 (1987).
[9] S. J. Sanders, P. M. Bellan, and R. A. Stern, Phys. Plasmas **5**, 716 (1998).
[10] M. J. Goeckner, J. Goree, and T. E. Sheridan, Phys. Fluids B **3**, 2913 (1991).
[11] G. D. Severn, Xu Wang, Eunsuk Go, and N. Hershkowitz, Phys. Rev. Lett. **90**, 145001 (2003).
[12] G. A. Hebner, J. Appl. Phys. **80**, 2624 (1996).
[13] N. Sadeghi, M. van de Grift, D. Vender *et al.*, Appl. Phys. Lett. **70**, 835 (1997).
[14] M. Tadokoro, H. Hirata, N. Nakano *et al.*, Phys. Rev. E **58**, 7823 (1998).
[15] G. A. Hebner and P. A. Miller, J. Appl. Phys. **87**, 8304 (2000).
[16] D. C. Zimmerman, R. McWilliams, and D. A. Edrich, Plasma Sources Sci. Technol. **14**, 581 (2005).
[17] E. E. Scime, P. A. Keiter, M. W. Zintl *et al.*, Plasma Sources Sci. Technol. **7**, 186 (1998).
[18] J. L. Kline, E. E. Scime, R. F. Boivin *et al.*, Phys. Rev. Lett. **88**, 195002 (2002).
[19] J. L. Kline, E. E. Scime, R. F. Boivin *et al.*, Phys. Plasmas **10**, 2127 (2003).

[20]X. Sun, C. Biloiu, R. Hardin, and E. E. Scime, Plasma Sources Sci. Technol. **13**, 359 (2004).
[21]T. Nakano, N. Sadeghi, and R. A. Gottscho, Appl. Phys. Lett. **58**, 458 (1990).
[22]N. Sadeghi, T. Nakano, D. J. Trevor, and R. A. Gottscho, J. Appl. Phys. **70**, 2552 (1991).
[23]T. Nakano, N. Sadeghi, D. J. Trevor *et al.*, J. Appl. Phys. **72**, 3384 (1992).
[24]S. H. Seo, J. I. Hong, K. H. Bai, and H. Y. Chang, Phys. Plasmas **6**, 614 (1999).
[25]www.plasmart.com
[26]K. Kadota and Y. Kaneko, Jpn. J. Appl. Phys. **13**, 1554 (1974).
[27]D. Leonhardt, C. R. Eddy Jr., V. A. Shamamian *et al.*, J. Appl. Phys. **83**, 2971 (1998).
[28]M. D. Kilgore, H. M. Wu, and D. B. Graves, J. Vac. Sci. Technol. B **12**, 494 (1994).